Fish and Shellfish Immunology 86 (2019) 858–867

Contents lists available at ScienceDirect

Fish and Shellfish Immunology

journal homepage: www.elsevier.com/locate/fsi

Full length article

Transcriptome profiles in the spleen of African catfish (*Clarias gariepinus*) challenged with *Aeromonas veronii*

Zhuanzhuan Li, Xiaomei Wang*, Chengxun Chen, Jinwei Gao, Aijun Lv

Tianjin Key Laboratory of Aqua-Ecology and Aquaculture, College of Fisheries, Tianjin Agricultural University, Tianjin, 300384, China

ARTICLE INFO

Keywords:
Clarias gariepinus
Spleen
RNA-seq
Transcriptome
Immune response
Aeromonas veronii

ABSTRACT

The African catfish, *Clarias gariepinus*, an important cultured freshwater species in many countries, possess the characteristic of high disease resistance. However, little genomic information for this character of the fish is available up to now. To address the shortfall and to better understand *C. gariepinus* immune response to pathogen infection at molecular level, *C. gariepinus* were challenged with potent *A. veronii* and the high-throughput RNA sequencing (RNA-seq) technology were employed to produce transcriptomes from spleen. In total, an average of 46,073,372 clean reads obtained were *de novo* assembled into 156,955 unigenes with an average length of 1082 bp. All of unigenes were annotated to seven public databases. Three comparisons were separately conducted between the infected groups at 3 h, 24 h, 48 h post-challenge and control group. A total of 2482 differentially expressed unigenes (DEGs) were identified. Among these, 114 immune-related DEGs were captured, including 88, 42, and 31 genes at 3 h, 24 h and 48 h after infection respectively, for analysis of expression pattern and enrichment. The 114 DEGs displayed four expression patterns by cluster analysis and they were significantly enriched in 38 pathways ($q < 0.01$) related to the immune or disease, five of which were NF-kappa B, TNF, NLR, TLR and RLR pathways. Finally, the expression levels of twelve selected immune-related DEGs involved in above five pathways were scrutinized. Seven of which were up-regulated at 3 h after infection, afterward, their expression dropped to control level. In summary, this study provides valuable transcriptome resource for understanding the defense mechanisms of *C. gariepinus* in resistance to pathogens from the gene expression viewpoint, which also open up the possibility to study the immune complexity and to better comprehend the interrelationships between some immune pathways in *C. gariepinus*.

1. Introduction

The African catfish, *Clarias gariepinus*, a member of the family Claridae, is native to the Nile valley of Africa and introduced to China from Egypt in 1981. This species is worldwide commercial freshwater fish due to fast growth, antihypoxia and high stocking density rearing, especially, it was considered to be less prone to disease in culture [1,2]. Precious reports in *C. gariepinus* predominantly focused on the growth performance, morphology as well as histochemistry and hematology effected by culture conditions such as stocking densities, feed and nitrogen content et al. [3–7]. However, no information on the mechanism of high disease resistance of *C. gariepinus* were reported at molecular level.

With the extensive increase in aquaculture, more researchers pay attention to the role of fish immune system defending against diseases. It is well known that an organism can successfully defend itself against diseases depending on the complex immune system by identifying and eliminating the invading pathogen [8,9]. Teleost fish possess both innate and acquired immune system, but the fish mainly rely on innate immune system to immediately prevent pathogens from entering organism [10]. In teleost fish, organs involved in immune response mainly consist of the lymphoid tissues, including kidney, spleen and thymus as well as mucosa-associated lymphoid tissues such as gut, skin and gills [11]. Of which, spleen is recognized as an essential immune organ involved in innate immunity and also a main target organ for pathogenic bacteria infection [12]. Recently, the high-throughput sequencing are widely used in transcriptome studies of various organisms, with or without their genome sequences [13]. The RNA-seq of spleen is of great significance for revealing the immune responses from the level of gene expression. Up to now, some studies have been investigated that the spleen transcriptomes at different time points in different fishes challenged with various pathogens, e.g. in Nile tilapia (*Oreochromis*

* Corresponding author.
E-mail addresses: zhuanzhuanlee@163.com (Z. Li), xiaomeiw@tjau.edu.cn (X. Wang), 489699261@qq.com (C. Chen), 56965198@qq.com (J. Gao), lajand@126.com (A. Lv).

https://doi.org/10.1016/j.fsi.2018.12.029
Received 27 August 2018; Received in revised form 10 December 2018; Accepted 15 December 2018
Available online 17 December 2018
1050-4648/

Abbreviations

NF-κB	Nuclear factor kappa B
TNF	Tumor necrosis factor
NLR	Nucleotide binding and oligomerization domain (NOD)-like receptor
TLR	Toll-like receptor
RLR	Retinoic acid-inducible gene (RIG)-like receptor
PRR	Pattern recognition receptor
LRR	Leucine-rich repeat
PAMP	Pathogen-associated molecular pattern
TIR	Toll- Interleukin-1 receptor
TRIF	TIR domain-containing adaptor inducing IFN-β
TRAM	TRIF-related adaptor molecule
MyD88	Myeloid differentiation factor 88
IRAK-4	Interleukin-1 receptor-associated kinase 4
TNFR	Tumor necrosis factor receptor
TRAF6	TNFR associated factor 6
TAK1	Transforming growth factor beta (TGF-β)-associated kinase 1
IKK	IκB kinase
IκBα	Inhibitor of nuclear factor-kappa B alph
IL	Interleukin
NALP	NACHT, LRR and PYD domains-containing protein
SGT1	Suppressor of the G2 allele of Skp1
ASC	Apoptosis-associated speck-like protein containing a CARD domain
cIAP	Cellular inhibitor of apoptosis
NIK	NF-κB-inducing kinase
TNFRSF	TNFR superfamily

niloticus) [14], grass carp (*Ctenopharyngodon idellus*) [15], half-smooth tongue sole (*Cynoglossus semilaevis*) [16] and orange-spotted grouper (*Epinephelus coioides*) [17], transcriptomes were conducted at 6 h, 6 h, 20 h and 48 h, respectively; transcriptomes of common carp (*Cyprinus carpio*) [18] and Ya-fish (*Schizothorax prenanti*) [12] were analyzed at 4, 12, 24 h and at 4, 24, 48 h, severally. Nevertheless, the knowledge of detailed molecular events happened in *C. gariepinus* during infection process is still deficient.

Aeromonas veronii is a gram-negative bacterium with rod-shaped and polar flagella in family Aeromonadaceae [19,20]. It causes several disease symptoms on farmed fish, for instance skin ulcer, swelling of tissues, enteritis, hemorrhagic septicemia even results high mortality of fish leading to the enormous economic losses [21–23].

In order to understand the vital roles of spleen in high disease resistance of *C. gariepinus*, we applied RNA-seq technology for analyzing the transcriptome differences of spleen from control and infection with *A. veronii* at 3 h, 24 h and 48 h without previously annotated genomes as references. Then, some immune-related differentially expressed genes (DEGs) were selected to further analyze their expression patterns as well as carry out GO and KEGG enrichment. Expression levels of some immune-related DEGs were scrutinized. The present study is the first to address the immune responses of the *C. gariepinus* to *A. veronii* infection at the transcriptome level, and it provides insight into the potential immune role of spleen in *C. gariepinus*.

2. Materials and methods

2.1. Fish and A. veronii challenge

Healthy *C. gariepinus* for the present study were obtained from Deren agricultural development co., Ltd, Tianjin, China. Prior to the bacterial infection, fish were raised in freshwater rearing tanks at 65 kg fish/m^3 depending upon our previous study [3,4] with temperature of 27 ± 1 °C for 10 days. Aeration was provided and Fish were fed with commercial catfish feed diet at 2.0% of body weight twice daily (08:00 and 16:00) during the trial. To mimic the practical water exchange, the 75% of water volume was renewed with aerated water (27 ± 1 °C) 2 h after each feeding. After adaptation, the fish weighing(63.84 ± 5.91)g were randomly chosen for next experiment.

The *A. veronii* (designated SG-1) was used for experimental infection. The initial bacteria, originating from diseased *Silurus soldatovi* liver, were isolated and purified, furthermore checked by gram staining, cell morphology, biochemical characteristics, molecular identification and infection experiment [22]. According to our preliminary challenge experiment in *C. gariepinus* and other researches [12,15,16,18], as infection groups, every fish were inoculated by intraperitoneal injection with *A. veronii* (suspended in sterile physiological saline) at a dose of 200 μL of 4×10^8 CFU/mL; while as control, fish were injected with sterile physiological saline at the same dosage.

2.2. Sampling

In tissues collection, the fish were randomly sampled at 3 h, 24 h and 48 h post-injection (hpi). Prior to dissecting, fish were anesthetized by an overdose of MS-222 then placed on ice, spleen were immediately snap frozen in liquid nitrogen and stored at −80 °C for RNA isolation. In order to obtain wide transcriptome coverage, spleen from six sampled individuals were pooled for total RNA isolation. One spleen pool from control group and three spleen pools from infection groups were denoted as CS, TS_3 h, TS_24 h and TS_48 h, respectively, corresponding to the sampling design.

2.3. RNA preparation, library construction and transcriptome sequencing

Total RNA were isolated with Trizol reagent (Tiangen, China) following the manufacturer's protocol. The quality of each RNA sample was monitored by agarose gel electrophoresis, the NanoPhotometer® spectrophotometer (IMPLEN, CA, USA) and Agilent Bioanalyzer 2100 system with RNA 6000 Nano Kit (Agilent Technologies, CA, USA). The concentration of each RNA sample was measured using Qubit® RNA Assay Kit in Qubit® 2.0 Flurometer (Life Technologies, CA, USA).

One and half micrograms RNA per sample were used for generating cDNA libraries. Sequencing libraries were constructed using NEBNext® Ultra™ RNA Library Prep Kit for Illumina® (NEB, USA) according to manufacturer's instructions, and index codes were added to attribute sequences to each sample. In brief, mRNA purification was performed via poly (dT) magnetic beads. The purified mRNA was fragmented and used for the synthesis of first strand cDNA using random hexamer primer, subsequently followed by the second strand cDNA synthesis, end repair and adapters ligation. The fragments were purified with AMPure XP system (Beckman Coulter, Beverly, USA) for selecting cDNA fragments of preferentially 150–200 bp in length. The mixtures of 3 μL USER Enzyme (NEB, USA) and the size-selected, adaptor-ligated cDNA were incubated at 37 °C for 15 min followed by 5 min at 95 °C before PCR. Then PCR was performed, amplicons were purified using AMPure XP system and quality of libraries was estimated on the Agilent Bioanalyzer 2100 system. The sequencing of each cDNA library was performed on an Illumina Hiseq 4000 platform and paired-end reads were generated.

2.4. De Novo assembly, functional annotation and classification

Raw reads of fastq format were firstly processed through in-house perl scripts. Clean reads were produced by removing reads containing adapter, uncertain 'N' nucleotides with the ratio of 'N' > 10% and low quality reads from raw reads. At the same time, Q-sources and GC-

content of the clean data were calculated. The high quality clean reads were used for transcriptome assembly using Trinity platform [24] with minimum k-mer coverage set to 2 by default and all other parameters set default for without reference genome. The longest transcript in one gene was regarded as unigene [25]. The function of unigenes were annotated depending upon following databases: Nr (NCBI non-redundant protein sequences), Nt (NCBI nucleotide sequences), PFAM (Protein Family), COG/KOG (Clusters of Orthologous Groups of proteins/euKaryotic Ortholog Groups), Swiss-Prot (A manually annotated and reviewed protein sequence database), KEGG (Kyoto Encyclopedia of Genes and Genomes) and GO (Gene Ontology). Furthermore, overall annotated unigenes were classified based on KOG, GO and KEGG databases, respectively.

2.5. Genes expression levels analysis, DEGs identification and validation

Gene expression levels of each sample were estimated by RSEM [26]. Prior to DEGs analysis, the read counts for each sequenced library were adjusted by edgeR program package through one scaling normalized factor. The DEGseq (2010) R package was used in order to analyze differential gene expression of two samples. P value was adjusted using q value [27]. The q value < 0.005 and $-1 > \log_2$ (fold change) > 1 was set as the threshold for significantly differential gene expression.

To validate the gene expression results of transcriptome data, some DEGs were randomly selected for real-time qPCR. Specific primer pairs (Table 1) for qPCR were designed using NCBI Primer 3-blast depending on the corresponding sequences provided in RNA-seq data. The qPCR were carried out in a final volume of 20 μL using PerfeCTa® SYBR® Green SuperMix following the instruction manual of the kit (Quanta biotech, USA) on an iQ™ 5 real-time PCR detection system (Bio-Rad, USA). Each qPCR reaction was performed in triplicate, the expression values of the ten genes were normalized with the reference gene (GAPDH), and expression levels were calculated using $2^{-\Delta\Delta CT}$ method. Using OriginPro9.1 software, a linear regression analysis was performed between data of qPCR and RNA-seq. Significance of difference between the two data were detected with the method of T-test by software SPSS17.0.

2.6. Analysis of DEGs in three comparisons

We separately conducted three comparisons between the infected groups at 3 h, 24 h, 48 h post-challenge and control group (namely TS_3 h vs CS, TS_24 h vs CS, TS_48 h vs CS), immune-related DEGs were captured from DEGs datasets, then subjected to GO enrichment and KEGG pathways analyses by using the GOseq R packages based Wallenius non-central hyper-geometric distribution [28] and KOBAS [29] software, respectively. The significance levels of all GO and KEGG terms were determined based on corrected P-value (i.e. q-value < 0.05).

3. Results and discussion

3.1. Sequencing, assembly and unigenes annotation

Four assembled libraries corresponding to 4 pooled spleen samples (CS, TS_3 h, TS_24 h and TS_48 h) of *C. gariepinus* were sequenced on an Illumina HiSeq 4000 platform and generated a total of 189,561,294 raw reads and 184,293,488 (97.22% of the raw reads) clean reads, and the quality of clean reads was assessed (Table 2). By using Trinity software suite, high quality clean reads were assembled into 263,825 transcripts with an average length of 758 bp, and 156,955 unigenes were produced with a size range of 201 bp to 27,035 bp and a N50 length of 1774 bp (Fig. 1), which was coincident with the N50 length of unigenes in channel catfish (*Ictalurus punctatus*), and yellow catfish (*Pelteobagrus fulvidraco*) and climbing perch (*Anabas testudineus*) [30–32], suggesting a good assemble quality of the transcriptome for *C. gariepinus* in current study. All clean data of the results of this article were available in the NCBI Sequence Read Archive database (https://www.ncbi.nlm.nih.gov/bioproject/PRJNA487132) under accession number PRJNA487132.

The functions of overall unigenes were annotated based on seven public databases, in which 69,832 unigenes had homologs in at least one database, and 15,070 had matched in all seven databases (Table 2). KOG is a database where orthologous gene products are classified. From the results of KOG annotation, 156,955 unigenes against KOG database yielded 26,423 putative proteins, fell into 26 groups including 1 unnamed protein group, of which 352 proteins were related to defense mechanisms. The GO analysis is an international standardized gene functional classification system, in present study, 46,385 unigenes were classified into biological process, cellular component and molecular function, which contained 25, 20 and 10 subcategories, respectively. In biological process, 6374 unigenes related to 'response to stimulus' (GO: 0050896) and 155 unigenes responded to 'immune system process' (GO: 0002376). 155 unigenes were mainly involved in the regulation of immune system process (103 unigenes), immune response (71 unigenes), immune effector process (37 unigenes) and leukocyte activation (30 unigenes), which may provide an explanation of defense mechanism in *C. gariepinus* spleen challenged with *A. veronii*. KEGG is a database to understand the advanced functions of biological systems via confirming the signaling pathway at the molecular level. In the current study, KEGG classification revealed that 26,588 unigenes were classified into 32 pathways at hierarchy 2. Signal transduction was the most abundant KEGG pathway (4407 unigenes, 16.57%), followed by immune system (2029 unigenes, 7.63%) and endocrine system (1921 unigenes, 7.23%). Our present annotation results provided an important and valuable database for future research on the specific traits of *C. gariepinus*.

3.2. Genes expression levels analysis, DEGs identification and validation

Genes expression levels were estimated using RSEM program, more than 74% clean reads of each sample were mapped onto the unigenes. Read count value of each gene was obtained from the mapping results (data not shown). 3741 DEGs were identified using DEGseq (2010) R package with q value < 0.005 and $|\log_2(\text{foldchange})| > 1$.

Table 1
Information of the primers for qPCR.

Gene name	Primer		Amplicon size (bp)
	Name	Sequence (5'—3')	
TLR1	TLR1-F	CCGATTCCTTTGTGCCTGAT	178
	TLR1-R	GCCAATGCCCTGTCCCTA	
TLR5	TLR5-F	GCCTGTCCAGTCTGACAACA	170
	TLR5-R	CTGCTCCAGAGACACAAGGG	
MyD88	MyD88-F	CTACTGCCAGAGCGACTT	179
	MyD88-R	CATCAGAAATGACCACCAC	
IκBα	IκBα-F	ACCGAGGATGGAGACACGTA	166
	IκBα-R	TGATGTGAGGCTGCTCTGTG	
NF-κB2 (p100)	NF-κB2-F	TACAGGACGAGAACGGAGACACG	136
	NF-κB2-R	TGGCTGAGGTGGTTGAACTTGTTG	
IL-8	IL-8-F	TCGCCGTATCGGGAAAATGA	126
	IL-8-R	GGTGCTTTAGGGTCCAGACA	
c-lys	c-lys-F	GCTAACTGGGTTTGCTTGGC	157
	c-lys-R	AGAGTTTGCACCCGTTAGCA	
g-lys	g-lys-F	CTGAGGGGAGCATGGAACAG	107
	g-lys-R	TGCTCTTTGGGCCAGTTAGG	
Hepcidin	Hepcidin-F	TGAGACTGCATCATTGGCGA	88
	Hepcidin-R	GCAGTATCGGCACATGGAGA	
Pardaxin	Pardaxin-F	TCTCCAGAGGTGGTGTGTCA	126
	Pardaxin-R	TCCATCCTGGTTGGGTAACG	
GAPDH	GAPDH-F	TGCAGGTCAATGAAGGGGTC	122
	GAPDH-R	ACCATGTCAGACCTTTGCGT	

Table 2
The transcriptome summary of *C. gariepinus*.

	Index	CS	TS_3 h	TS_24 h	TS_48 h
Sequence statistics	Raw Reads	48987506	46530792	50414104	43628892
	Clean reads	47818068	45544268	48721478	42209674
	Clean bases (bp)	7.17G	6.83G	7.31G	6.33G
	Error rate of base (%)	0.02	0.02	0.02	0.02
	> Q20 of clean reads(%)	96.63	96.74	96.83	95.76
	> Q30(%)	91.92	92.16	92.36	89.84
	GC(%)	46.60	46.44	46.26	46.52
Assembling statistics	Number of transcripts	263825			
	Number of unigenes	156955			
Annotation statistics	Number in NR	54042 (34.43%)			
	Number in NT	43699 (27.84%)			
	Number in PFAM	45899 (29.24%)			
	Number in KOG	26423 (16.83%)			
	Number in SwissProt	42535 (27.10%)			
	Number in KEGG	26588 (16.93%)			
	Number in GO	46385 (29.55%)			
	Number in all Databases	15070 (9.60%)			
	Number in at least one Database	69832 (44.49%)			
	Total Number	156955 (100%)			

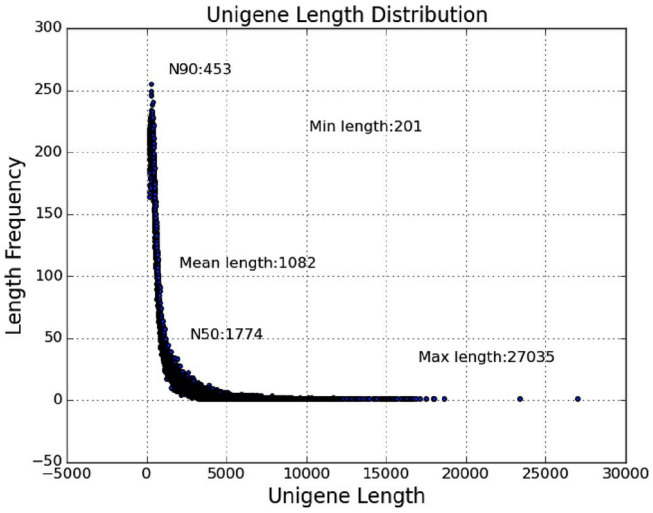

Fig. 1. Length distribution of the assembled unigenes. X-axis indicates the unigene length (bp), Y-axis indicates the number of unigenes of each length. N50/N90: All of unigenes are sorted and added one by one from long to short, when the accumulated length is just longer than or equal to 50%/90% of the sum of the lengths of all unigenes, the length of the shortest unigene is defined as N50/N90, respectively.

To confirm the gene expression results obtained from RNA-seq data, randomly selected ten immune-related DEGs were validated using qPCR technology, the results showed that qPCR data is a positive linear correlation with RNA-seq data, R = 0.804 (Fig. 2), and there was no statistically significant difference between the two datasets (T-test $P > 0.05$). This result resembled those of *A. testudineus*, *C. idella* and *C. semilaevis* [32–34], indicating that RNA-seq in our study was a reliable reference for expression profiling study.

3.3. Analysis of all of DEGs in three comparisons

In this paper, 2482 DEGs were detected in three transcriptome comparisons, among these, a total of 1878 (containing 989 up-regulated and 889 down-regulated genes), 779 (423 and 356) and 549 DEGs (285 and 264) were differentially expressed at 3 h, 24 h, and 48 h after challenge compared with the control group, respectively (Fig. 3). The number of DEGs was decreased over a 48 h period, as can be seen the genes activated were the most at the early stage of infection and it revealed that *C. gariepinus* spleen was rapid response to *A. veronii*. There were 1149 and 638 DEGs were identified in *O. niloticus* spleen at 5 h, 50 h following *Streptococcus iniae* challenge [35]. On the contrary, the DEGs number of *S. prenanti* spleen were increased from three time points within 4 h–48 h [12]. In immersion exposure, after *A. hydrophila* infection of blue catfish (*I. furcatus*) skin, the number of DEGs were declined during 2 h–24 h [36], whereas at 3 h, 24 h and 72 h post-challenged with *Edwardsiella ictaluri* in *I. punctatus* intestinal tracts DEGs number reached to peak at 72 h [30]. These results indicated that different species, organs, infection methods and pathogens lead to differences in change trend of DGEs number.

3.4. Analysis of immune-related DEGs in three comparisons

3.4.1. Analysis of expression patterns in immune-related DEGs

In order to investigate spleen immunity response to *A. veronii*, immune-related DEGs were further counted, and 114 immune-related

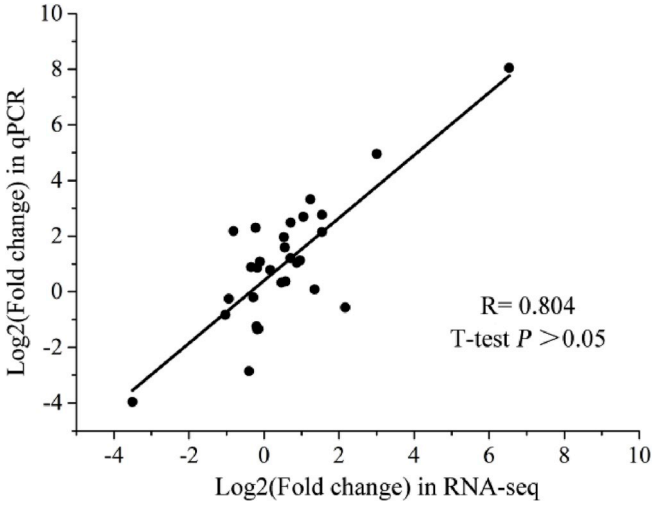

Fig. 2. Correlation results between RNA-seq and qPCR data. In qPCR analyses, the expression levels were normalized to GAPDH, each point represents a value of fold change of expression level between treatments and control group or between two treatments from RNA-seq (x-axis) and qPCR (y-axis) data. Fold-change values were log2 transformed.

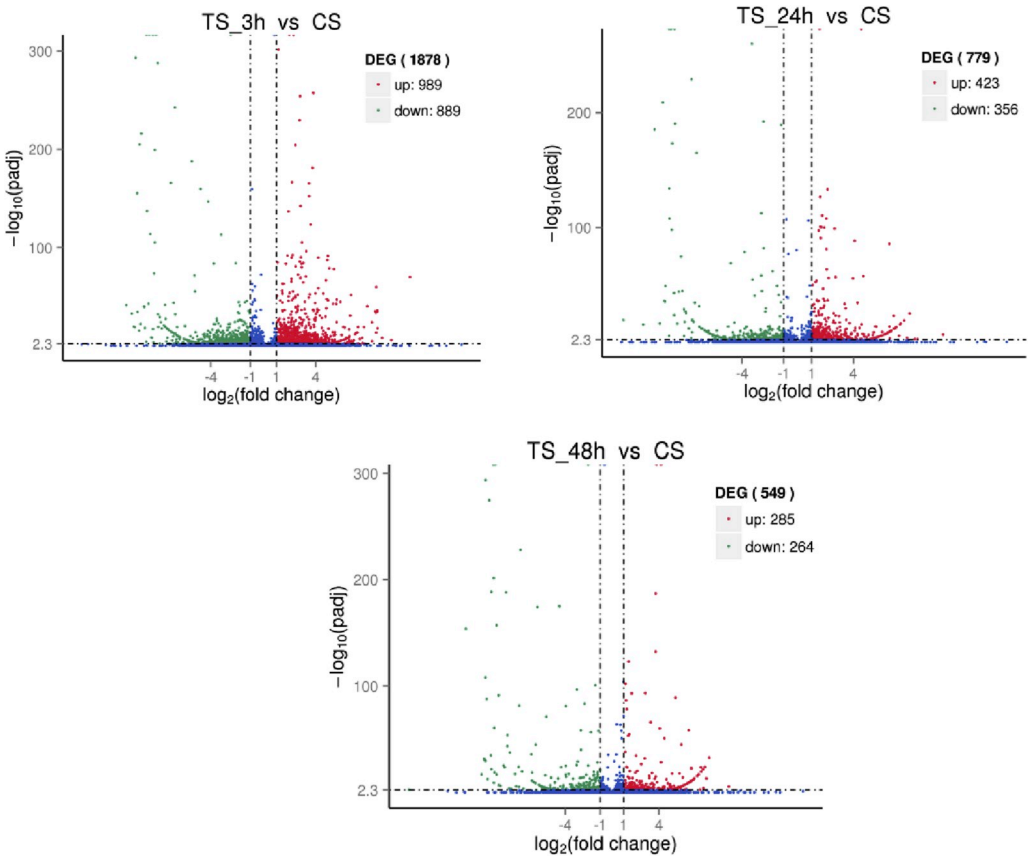

Fig. 3. Volcano Plot of differentially expressed genes (DEGs) in three comparisons upon *A. veronii*. X-axis exhibits change in fold between two sets of samples (TS_3 h vs CS, TS_24 h vs CS and TS_48 h vs CS) and Y-axis shows significance of DEGs. Red (up-regulation) and green (down-regulation) dots indicate significantly different expression (q-value < 0.005, |log2 (fold change)| > 1), respectively, and dots in blue color show no significant differences. (For interpretation of the references to color in this figure legend, the reader is referred to the Web version of this article.)

DEGs were discovered among three comparisons. Venn diagram analysis revealed that there were 88 (65 up-regulated and 23 down-regulated), 42 (24 and 18), and 31 (18 and 13) genes at 3, 24 and 48 hpi compared with control group, respectively, some information were shown in Fig. 4. Twelve genes were shared by three comparisons including 4 up-regulated and 8 down-regulated genes. It can be seen that the largest number of immune-related DEGs was at 3 h and that numbers were on the decline as time goes on. Moreover, at 3 h, the number of up-regulated genes was more than twice as many as that of down-regulated genes. However, at 24 and 48 h, the number of them was roughly equivalent. It showed that the immune response was particularly obvious at 3 hpi.

In the hierarchical cluster analysis, 114 immune-related DEGs in TS_48 h, CS and TS_24 h were firstly fell into one group, then TS_3 h genes were clustered with them together, indicating that expression changes of 114 immune-related DEGs at 3 hpi were the biggest differences compared with other two time points (Fig. 5). In terms of the expression patterns, these 114 genes were allocated into four clusters representing four different expression patterns (Fig. 5). It's worth noting that 67 (58.77%) genes were gathered in the cluster II, in which genes were relatively highly expressed at 3 h. While, in the cluster IV, most genes were relatively low expression at 3 h.

3.4.2. GO, KEGG enrichment analysis in immune-related DEGs

To determine the functional significance of the transcriptional changes in *C. gariepinus* response to infection, GO and KEGG enrichment were implemented for 114 immune-related DEGs. In this study, GO enrichment analysis revealed that 38 sub-categories were significantly enriched (q < 0.01) under the three major categories, i.e. biological process, cellular component and molecular function. Among of 38 GO terms, immune system process (GO: 0002376) and immune response (GO: 0006955) were the top 2 significantly enriched (q = 5.43E-32 and q = 3.53E-31) (Fig. 6). We also found that, in TS_3 h vs CS comparison, not only the enriched sub-categories were the most in all the three major categories, but the genes number of enriched sub-categories were also the most (Supplementary Tables 1–3). According to the results of heat map data and GO enrichment analysis, 114 immune-related DEGs involved in GO terms, immune system process and immune response, were enriched in cluster II, where gene expression were increased at 3 h but dropped to control level subsequently, suggesting that upon *A. veronii* infection, these genes play a pivotal role in defensing and resisting the attachment and infection of pathogen at early stage.

KEGG enrichment results showed 114 genes were classified into 38 signaling pathways (q < 0.01), five of which were obviously relevant

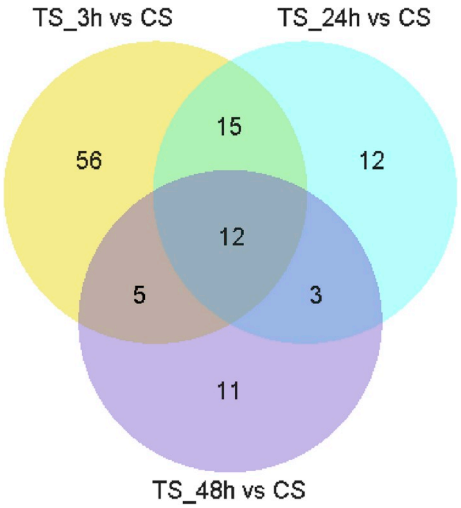

Fig. 4. Venn diagram analysis of immune-related DEGs upon *A. veronii*. Venn diagram shows the number of shared and specific DEGs among three comparisons (TS_3 h vs CS, TS_24 h vs CS and TS_48 h vs CS).

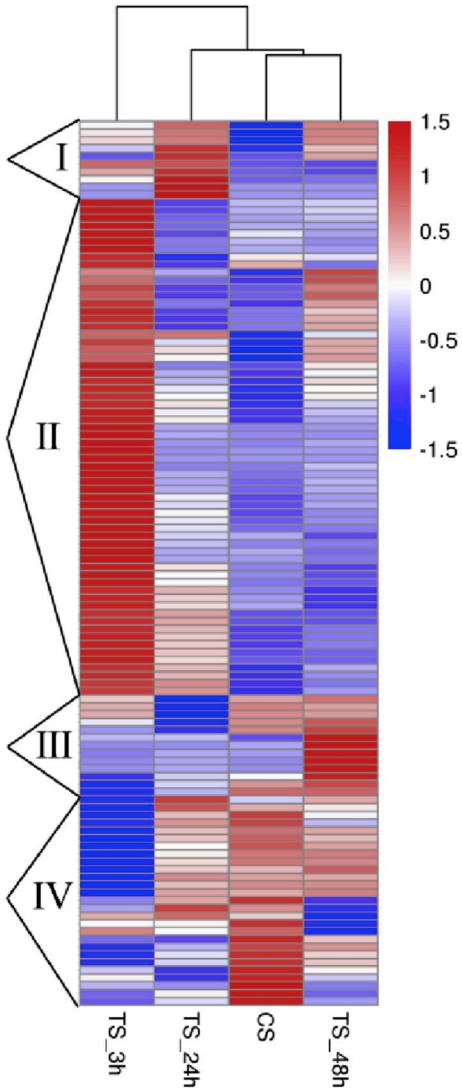

Fig. 5. Hierarchical cluster analysis of immune-related DEGs upon *A. veronii*. The scale shows the level of DEGs: high and low expression level of mRNA were shown in red and blue color, respectively. (For interpretation of the references to color in this figure legend, the reader is referred to the Web version of this article.)

to innate immune response, they were NF-κB signaling pathway (ko04064) (22 genes, 19.30%), TNF signaling pathway (ko04668) (22, 19.30%), NLR signaling pathway (ko04621) (12, 10.53%), TLR signaling pathway (ko04620) (15, 13.16%), and RLR signaling pathway (ko04622) (11, 9.65%). In the following, the aforesaid five pathways were further investigated to elucidate the details about the immune response to *A. veronii* infection from perspective of gene expression profiles (Fig. 7).

3.4.3. Pathway analysis

TLRs, the first PRRs to be characterized, are critical to the initiation of innate immune responses and comprises of three parts: an N-terminal ectodomain with LRR that are required for recognition of PAMPs, a transmembrane region, and a C-terminal cytoplasmic TIR domain that binds adaptor molecules and then activates downstream signaling pathways [37]. TLR1 and TLR5 are two of the TLRs locating on the cell membrane. TLR1 recognises bacterial peptidoglycan and lipoproteins in concert with TLR2, whereas TLR5 recognises bacterial flagellin expressed by flagellated bacteria [38,39]. In present experiment, transcriptomic profile analysis showed that the TLR5 were significantly up regulated at 3 hpi, but then declined to almost basal level (control group) at 24 and 48 hpi (Fig. 7). But, in blunt snout bream (*Megalobrama amblycephala*) challenged with *A. hydrophila* at 4 h, 12 h and 24 h, transcriptomic analysis in spleen revealed that expression of TLR5 were up at 4 h and 12 h then was down at 24 h [40]. Using qPCR technique, in *M. amblycephala* spleen after *A. hydrophila* challenge, significant increase of TLR5 expression at 12 h and 24 h as well as decrease at 48 h were observed, respectively [41]. The same phenomenon was also found in infection of *Pangasianodon hypophthalmus* with *E. tarda*, which caused an initial upregulation of TLR5 expression in spleen at 3 h, then quickly upregulated at 6 h and 12 h, ultimately rapidly down-regulated to the control level at 24 h and 48 h [42]. However, there was difference in *I. punctatus* spleen after infection with the ciliate parasite *Ichthyophthirius multifiliis*, the expressions of TLR5 were no significant changes at 6 h, 12 h, 24 h and 48 h [43]. These findings collectively reflected that TLR5 plays a fundamental role in the host innate immune response to bacteria. In *C. gariepinus*, significant down regulation of TLR1 was observed at 3 hpi, then returned to control level at 24 and 48 hpi (Fig. 7). Similarly, *O. niloticus* challenged with gram-positive *Streptococcus agalactiae*, TLR1 expression was decreased in spleen and kidney at 6 h [14]. While TLR1 expression in the spleen of *M. amblycephala* infected with *A. hydrophila* was up-regulated at 12 h post infection, later returned to the control level at 24 h, finally significantly down-regulated at 48 h [41]. Previous study found that infection of *I. punctatus* with *I. multifiliisq* caused obvious up-regulation of TLR1 expression of spleen at 12 hpi, then there were not remarkable differences at 6 h, 24 h and 48 h [43]. The different expression profiles of TLR1 implicated that respond of TLR1 to infections appears to be related with species of host and pathogen. Taken together, apparent expression changes of TLR1 and TLR5 indicated they were involved in recognition for *A. veronii* in spleen of *C. gariepinus* at the early stages.

TLR pathways rely on different adaptor molecules, e.g. MyD88, TIRAP, TRIF and TRAM [44]. In our study, only the MyD88 expression was significantly different. MyD88 consist of a TIR domain and a death domain (DD). Subsequently, MyD88 interact with IRAK-4, which active IRAK-1 and IRAK-2, then IRAKs dissociate from MyD88 and interact with TRAF6 [45]. Here, under recognition of *A. veronii*, the expression patterns of MyD88 and TRAF6 were similar to which of TLR5, whereas the range of their upregulation were smaller than that of TLR5 at 3 hpi (Fig. 7). This result was partly consistent with the analysis in *S. prenanti* challenged with *A. hydrophila,* in which MyD88 and TRAF6 expression in spleen was upregulated at 4 h, but MyD88 and TRAF6 were respectively downregulated at 48 h and 24 h [12]. It illustrated that downstream genes of TLR pathway were activated during the early infection events.

In addition, researchers have proved that MyD88-dependent NF-κB pathway exists when responded to stimulation [40,46]. Once immune signals are transduced from MyD88 to TRAF6, TRAF6 will response to TAK1 and IKK, subsequently IκBα was phosphorylated by activated IKK and degraded via ubiquitin mediation, finally NF-κB is dissociated, causing activation of the NF-κB pathway (also be called canonical NF-κB pathway). The activated NF-κB translocates into the nucleus where it bind to the specific regions of target genes, IκBα and downstream proinflammatory cytokines genes (for instance TNF-α, IL-1β, IL-6, IL-8 and IL-12), and promotes or enhances their expression [46–48]. It is worthy to be mentioned that in this experiment at 3 hpi the expression of IκBα was significantly up regulated, nevertheless, NF-κB was no changing, furthermore, IL-1β and IL-8 were found to be highly expressed significantly, whereafter they all returned to basal level at 24 and 48 hpi, except IL-1β was still significantly up regulated at 24 hpi (Fig. 7). The prior study unveiled that NF-κB pathway exists an autoregulatory loop, of which, positive feedback regulation can facilitate amplification of inflammatory signals, where activation of NF-κB strengthen the transcription of TNF-α and IL-1β, and both of them are in turn to active NF-κB via TNFRs and IL-1R. However, in negative feedback regulation, NF-κB activation result in transcription increase of

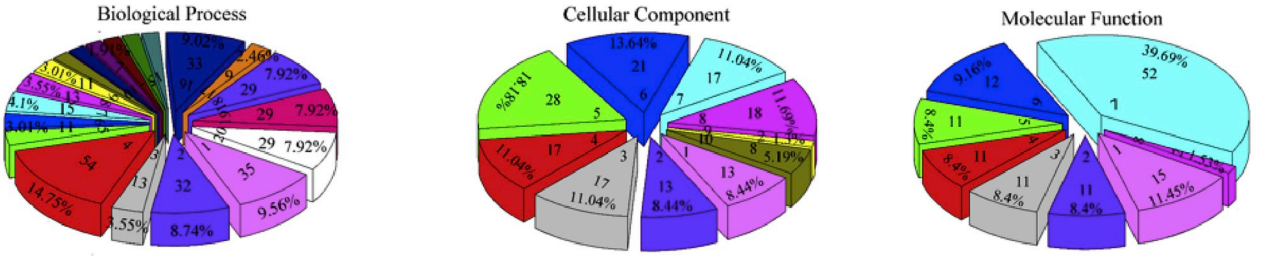

	GO term in biological process	q Value
1	immune system process	5.43E-32
2	immune response	3.53E-31
3	antigen processing and presentation	5.67E-19
4	response to stimulus	2.08E-12
5	chemotaxis	1.17E-07
6	taxis	1.17E-07
7	response to external stimulus	2.64E-07
8	response to chemical	3.13E-04
9	locomotion	9.12E-04
10	ubiquitin-dependent protein catabolic process	1.51E-03
11	modification-dependent protein catabolic process	1.51E-03
12	modification-dependent macromolecule catabolic process	1.51E-03
13	cellular protein catabolic process	2.41E-03
14	proteolysis involved in cellular protein catabolic process	2.41E-03
15	protein catabolic process	5.30E-03
16	cellular response to stimulus	5.63E-03
17	defense response	7.98E-03
18	signal transduction	7.98E-03
19	single organism signaling	8.44E-03
20	signaling	8.71E-03

	GO term in cellular component	q Value
1	MHC class II protein complex	1.29E-19
2	MHC protein complex	1.29E-19
3	plasma membrane protein complex	1.43E-12
4	plasma membrane part	4.04E-10
5	extracellular region	2.35E-09
6	cell periphery	1.91E-08
7	plasma membrane	3.56E-07
8	membrane protein complex	9.43E-04
9	interleukin-1 receptor complex	4.47E-03
10	extracellular space	6.84E-03

	GO term in molecular function	q Value
1	cytokine receptor binding	6.68E-14
2	chemokine activity	8.18E-13
3	chemokine receptor binding	8.18E-13
4	G-protein coupled receptor binding	3.76E-12
5	cytokine activity	7.51E-12
6	receptor binding	3.09E-06
7	protein binding	1.51E-03
8	interleukin-1 receptor binding	4.47E-03

Fig. 6. GO Enrichment analysis of immune-related DEGs upon *A. veronii*. Significantly enriched ($q < 0.01$) sub-categories were listed in biological process, cellular component and molecular function, severally. Number and its percentage of DEGs enriched in sub-categories were shown in each pie.

IκBα genes, which associates with NF-κB in the nucleus and brings the latter into the cytoplasm then suppress the activation of the NF-κB, ultimately terminate new cytokine transcription and limit the inflammatory response [47–49]. So in our data, on the one hand, activated NF-κB can keep certain stability in magnitude via positive and negative feedback regulation, which may explain why NF-κB expression was no changing. On the other hand, although IκBα was overexpressed, IL-1β and IL-8 were also highly expressed, which maybe regulated by other cross talk biological processes such as RLR and NLR pathway (Fig. 7). In particular, the later do not depend on the NF-κB pathway to trigger the production of proinflammatory cytokines (Fig. 7). In NLR pathway, the domain organization of NALPs includes (a) an N-terminal or pyrin domain (PYD); (b) a central NOD domain mediating self-oligomerization; and (c) a C-terminal LRR [50,51]. HSP90, an important molecular chaperone, can regulate many signaling proteins. Published reports have demonstrated that the presence of active HSP90 serve to SGT1 interaction with NALP3, subsequently cause recruitment of ASC and caspase-1, eventually activation of caspase-1 participate in the processing of IL-1β and IL-18 [52,53]. In our data, HSP90 were overexpressed significantly until 24 hpi, we speculated that up regulated HSP90 enhanced expression of IL-1β gene at 3 hpi (Fig. 7), which was consistent with the observed findings in *O. niloticus* [14].

IL-1β is regarded as an essential early response pro-inflammatory cytokine that can active a lot of cell type, either alone or in combination with other cytokines cope with the infection, injury and immunologic challenge [54]. IL-8 is a one of the first CXC chemokine, functional analysis displayed that IL-8 can be induced by inflammatory signals (e.g., TNF-α, IL-1β), chemical and environmental stresses, and steroid hormones [55]. After bacterial infection, the overexpressed IL-1β and IL-8 in *C. gariepinus* (Fig. 7) and other fishes were found. Prior study suggested that in large yellow croaker (*Pseudosciaena crocea*) spleen challenged with *A. hydrophila*, IL-1β and IL-8 were sharply expressed at 12 h [56]. *A. salmonicida* infection led to a dramatic increase in the expression of IL-1β during 1–4 h periods, later slowly increased at 24 h in zebrafish spleen [57]. As can be seen, the upregulation of these proinflammatory cytokines strongly suggests that the proinflammatory response may represent an important antibacterial mechanism at the early phase of infection.

In the canonical pathway, aside from the induction of mentioned TLR1, TLR5 and IL-1R, NF-κB pathway was also stimulated through TNFRs, such as TNFR2 directly binds to TRAF2 then recruits cIAP1/2, TLR1, TLR5 and IL-1R can recruit MyD88, both trigger downstream signaling events [58,59]. In present study, the expression of TRAF2 was significantly up at 3 hpi, then was down at 24 hpi, however the expression patterns of cIAP1 was consistent with which of MyD88 (Fig. 7). All of these findings unveiled that the NF-κB pathway was actived by the various signals.

Noncanonical pathway, one is called p100-mediated pathway, was induced by TNFs and sequentially activates NIK and IKK1. p100 was phosphorylated by IKKα and partially hydrolyzed to produce p52, which translocates into the nucleus with RelB [60]. p52 is an essential regulatory factor that participate in the maintenance of the peripheral B cell population, humoral responses, and normal spleen architecture. [61]. Our results displayed that the expression of p100 (p52) were increased significantly at 3 hpi (Fig. 7), which will contribute to explore the acquired immune response of *C. gariepinus* to *A. veronii*.

In summary, expression of twelve genes involved in NF-κB, TNF, NLR, TLR and RLR signaling pathways were analyzed in our study. Of which, 7 genes (TLR5, MyD88, TRAF2, IκBα, IL-8, cIAP1 and p100) were significantly up-regulated, on the contrary TLR1 and TNFR2 were significantly down regulated at 3 hpi in *C. gariepinus* spleen, afterward, their expression dropped to control level; however the significant up-regulation of IL-1β and HSP90 genes were observed at 3 and 24 hpi, TRAF2 was significantly up and down at 3 and 24 hpi, severally, then

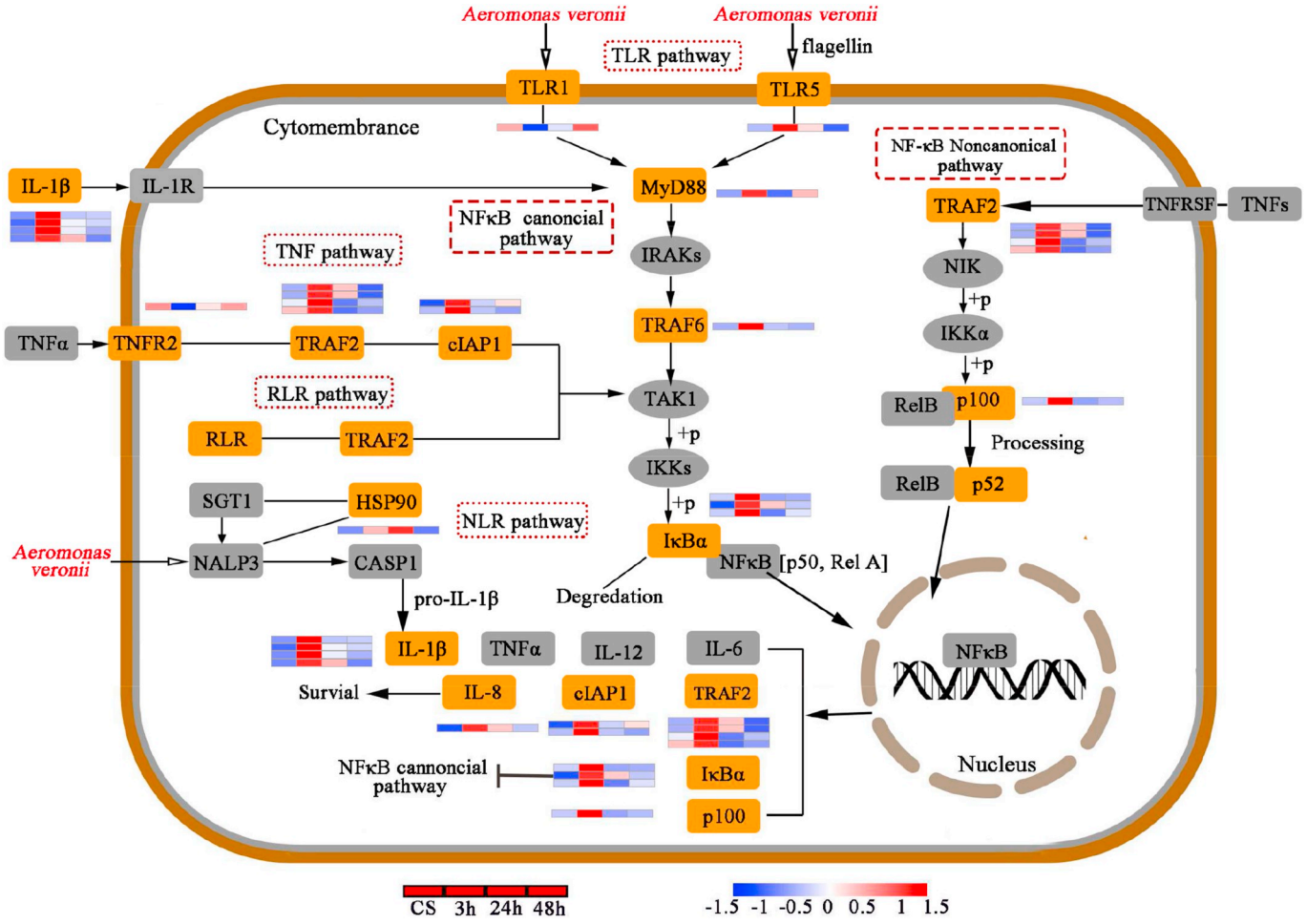

Fig. 7. KEGG pathway analysis of immune-related DEGs upon *A. veronii*. Five pathways i.e. NF-κB pathway, TNF pathway, NLR pathway, TLR pathway and RLR pathway were briefly shown in Fig. 7. The arrows represent the signaling directions. DEGs were highlighted with orange, while non-DEGs in our three comparisons were shown in gray. The expression patterns of DEGs were given next to the relative DEGs. (For interpretation of the references to color in this figure legend, the reader is referred to the Web version of this article.)

they all returned to the control level. These findings suggested that *C. gariepinus* defense and resist the attachment and infection of pathogen at early stage, we speculated that it was a reason of high disease resistant in *C. gariepinus*.

4. Conclusions

To our knowledge, for the first time, spleen transcriptome databases of *C. gariepinus* infected and non-infected by *A. veronii* were acquired, in which, abundant DEGs were found and some immune-related DEGs were further analyzed. In our study, although genes analysis involved in NF-κB, TNF, NLR, TLR and RLR signaling pathways were limited, our results improve understanding of the immune mechanisms of *C. gariepinus* in response to *A. veronii*. For this reason, more significant genes involved in immune responses need to be further analyzed, the novel transcriptome data obtained open up the possibility for this work.

Conflicts of interest

The authors declare no conflicts of interest.

Acknowledgements

The study was funded by the Natural Science Foundation of Tianjin, China [grant numbers 15JCZDJC33500, 16JCZDJC33500] and was partially by the Science and Technology Planning Project of Tianjin, China [grant number 16ZXZYNC00090]. We thank our colleague Professor Aijun Lv for providing us the pathogenic bacterium, *A. veronii* and precious advice on challenge experiment.

Appendix A. Supplementary data

Supplementary data to this article can be found online at https://doi.org/10.1016/j.fsi.2018.12.029.

References

[1] J.R.S. Vitule, S.C. Umbria, J.M.R. Aranha, Introduction of the African catfish *Clarias gariepinus* (BURCHELL, 1822) into southern Brazil, Biol. Invasions 8 (4) (2006) 677–681, https://doi.org/10.1007/s10530-005-2535-8.

[2] By M. Prokešová, B. Drozd, J. Kouřil, V. Stejskal, J. Matoušek, Effect of water temperature on early life history of African sharp-tooth catfish, *Clarias gariepinus* (Burchell, 1822), J. Appl. Ichthyol. 31 (S 2) (2015) 18–29, https://doi.org/10.1111/jai.12849.

[3] W. Dai, X.M. Wang, Y.J. Guo, Q. Wang, J.H. Ma, Growth performance, hematological and biochemical responses of African catfish (*Clarias gariepinus*) reared at different stocking densities, Afr. J. Agric. Res. 6 (28) (2011) 6177–6182, https://doi.org/10.5897/AJAR11.1278.

[4] X.M. Wang, W. Dai, M. Xu, B.P. Pan, X.Q. Li, Y.T. Chen, Effects of stocking density on growth, nonspecific immune response, and antioxidant status in African catfish (*Clarias gariepinus*), Isr. J. Aquacult-Bamid. 65 (2) (2013) 195–204.

[5] M. Besson, H. Komen, J. Aubin, I.J.M. de Boer, M. Poelman, E. Quillet, C. Vancoillie, M. Vandeputte, J.A.M. van Arendonk, Economic values of growth and feed efficiency for fish farming in recirculating aquaculture system with density and nitrogen output limitations: a case study with African catfish (*Clarias gariepinus*), J. Anim. Sci. 92 (12) (2014) 5394–5405, https://doi.org/10.2527/jas.2014-8266.

[6] I. Putra, R. Rusliadi, M. Fauzi, U.M. Tang, Z.A. Muchlisin, Growth performance and feed utilization of African catfish *Clarias gariepinus* fed a commercial diet and reared in the biofloc system enhanced with probiotic, F1000 Res. 6 (2017) 1545–1553, https://doi.org/10.12688/f1000research.12438.1.

[7] A.A. Raji, P.A. Alaba, I. Yusuf, N.H.A. Bakar, N.H.M. Taufek, H. Muin, Z. Alias, P. Milow, Fishmeal replacement with Spirulina Platensis and Chlorella vulgaris in African catfish (*Clarias gariepinus*) diet: effect on antioxidant enzyme activities and haematological parameters, Res. Vet. Sci. 119 (2018) 67–75, https://doi.org/10.1016/j.rvsc.2018.05.013.

[8] B. Magnadottir, Immunological control of fish diseases, Mar. Biotechnol. 12 (4) (2010) 361–379, https://doi.org/10.1007/s10126-010-9279-x.

[9] A.E. Ellis, Innate host defense mechanism of fish against viruses and bacteria, Dev. Comp. Immunol. 25 (8–9) (2001) 827–839, https://doi.org/10.1016/S0145-305X(01)00038-6.

[10] P.R. Rauta, B. Nayak, S. Das, Immune system and immune responses in fish and their role in comparative immunity study: a model for higher organisms, Immunol. Lett. 148 (1) (2012) 23–33, https://doi.org/10.1016/j.imlet.2012.08.003.

[11] C.Mcl. Press, Ø. Evensen, The morphology of the immune system in teleost fishes, Fish. Shellfish Immunol. 9 (4) (1999) 309–318.

[12] H. Ye, S.J. Xiao, X.Q. Wang, Z.Y. Wang, Z.S. Zhang, C.K. Zhu, B.J. Hu, C.H. Lv, S.M. Zheng, H. Luo, Characterization of spleen transcriptome of *Schizothorax prenanti* during *Aeromonas hydrophila* infection, Mar. Biotechnol. 20 (2) (2018) 1–11, https://doi.org/10.1007/s10126-018-9801-0.

[13] X. Li, Y. Kong, Q.Y. Zhao, Y.Y. Li, P. Hao, De novo assembly of transcriptome from next-generation sequencing data, Quant. Biol. 4 (2) (2016) 94–105, https://doi.org/10.1007/s40484-016-0069-y.

[14] R. Zhang, L.L. Zhang, X. Ye, Y.Y. Tian, C.F. Sun, M.X. Lu, J.J. Bai, Transcriptome profiling and digital gene expression analysis of Nile tilapia (*Oreochromis niloticus*) infected by *Streptococcus agalactiae*, Mol. Biol. Rep. 40 (10) (2013) 5657–5668, https://doi.org/10.1007/s11033-013-2667-3.

[15] Y. Yang, H. Yu, H. Li, A.L. Wang, Transcriptome profiling of Grass carp (*Ctenopharyngodon idellus*) infected with *Aeromonas hydrophila*, Fish Shellfish Immunol. 51 (2016) 329–336, https://doi.org/10.1016/j.fsi.2016.02.035.

[16] X. Zhang, S.L. Wang, S.L. Chen, Y.D. Chen, Y. Liu, C.W. Shao, Q.L. Wang, Y. Lu, G.Y. Gong, S.X. Ding, Z.X. Sha, Transcriptome analysis revealed changes of multiple genes involved in immunity in Cynoglossus semilaevis during Vibrio anguillarum infection, Fish Shellfish Immunol. 43 (1) (2015), https://doi.org/10.1016/j.fsi.2014.11.018 29-218.

[17] Y.H. Huang, X.H. Huang, Y. Yan, J. Cai, Z.L. Ouyang, H.C. Cui, P.R. Wang, Q.W. Qin, Transcriptome analysis of orange-spotted grouper (*Epinephelus coioides*) spleen in response to Singapore grouper iridovirus, BMC Genomics 12 (1) (2011) 556, https://doi.org/10.1186/1471-2164-12-556.

[18] Y.L. Jiang, S.S. Feng, S.H. Zhang, H. Liu, J.X. Feng, X.D. Mu, X.W. Sun, P. Xu, Transcriptome signatures in common carp spleen in response to *Aeromonas hydrophila* infection, Fish Shellfish Immunol. 57 (2016) 41–48, https://doi.org/10.1016/j.fsi.2016.08.013.

[19] H. Li, Study on Biochemical Activity and Pathogenicity of Extracellular Products of *Aeromonas veronii* from Channel Catfish (In Chinese), Sichuan Agricultural University, Cheng du, 2013.

[20] Y.S. Deng, J. Fang, J. Wang, L. Zhou, R. Zhu, Isolation and identification of a pathogenic bacterium *Aeromonas veronii* from diseased allogenic sliver crucian carp (in Chinese), Chin. J. Fish. 28 (2) (2015) 1–5, https://doi.org/10.3969/j.issn.1005-3832.2015.02.001.

[21] X.L. Huang, C.Y. Wu, Y.Q. Deng, K.Y. Wang, Y. Geng, J.Q. Zhao, Pathohistological observation of Ictalurus punctatus infected with *Aeromonas veronii* (in Chinese), Chin. Vet. Sci. 40 (7) (2010) 738–742, https://doi.org/10.16656/j.issn.1673-4696.2010.07.022.

[22] M.Y. Lu, X.C. Hu, A.J. Lv, J.F. Sun, C.X. Chen, X.M. Wang, Y.Y. Sung, Y.J. Song, Isolation, identification and susceptibility of *Aeromonas veronii* from diseased northern sheatfish *Silurus soldatovi* (in Chinese), J. Dalian Ocean Univ. 32 (5) (2017) 563–567, https://doi.org/10.16535/j.cnki.Dlhyxb.2017.05.010.

[23] Y. Liu, R. Yang, Y.Y. Chen, M.J. Song, Q.G. Yan, Q. Gong, Q. Li, H.C. Yang, J.S. Lai, Isolation,identification of *Aeromonas veronii* in *Acipenser dabryanus* and its histological observations (in Chinese), J. South. Agric. 49 (6) (2018) 1235–1241, https://doi.org/10.3969/j.issn.2095-1191.2018.06.28.

[24] M.G. Grabherr, B.J. Haas, M. Yassour, J.Z. Levin, D.A. Thompson, I. Amit, X. Adiconis, L. Fan, R. Raychowdhury, Q.D. Zeng, Z.H. Chen, E. Mauceli, N. Hacohen, A. Gnirke, N. Rhind, F.D. Palma, B.W. Birren, C. Nusbaum, K. Lindblad-Toh, N. Friedman, A. Regev, Full-length transcriptome assembly from RNA-Seq data without a reference genome, Nat. Biotechnol. 29 (7) (2011) 644–652, https://doi.org/10.1038/nbt.1883.

[25] B.J. Haas, A. Papanicolaou, M. Yassour, M. Grabherr, P.D. Blood, J. Bowden, M.B. Couger, D. Eccles, B. Li, M. Lieber, M.D. MacManes, M. Ott, J. Orvis, N. Pochet, F. Strozzi, N. Weeks, R. Westerman, T. William, C.N. Dewey, R. Henschel, R.D. LeDuc, N. Friedman, A. Regev, De novo transcript sequence reconstruction from RNA-seq using the Trinity platform for reference generation and analysis, Nat. Protoc. 8 (8) (2013) 1494–1512, https://doi.org/10.1038/nprot.2013.084.

[26] B. Li, C.N. Dewey, RSEM: accurate transcript quantification from RNA-Seq data with or without a reference genome, BMC Genomics 12 (2011) 323–338, https://doi.org/10.1186/1471-2105-12-323.

[27] J.D. Storey, R. Tibshirani, Statistical significance for genomewide studies, PNAS 100 (16) (2003) 9440–9445, https://doi.org/10.1073/pnas.1530509100.

[28] M.D. Young, M.J. Wakefield, G.K. Smyth, A. Oshlack, Gene ontology analysis for RNA-seq: accounting for selection bias, Genome Biol. 11 (2) (2010) R14–R25, https://doi.org/10.1186/gb-2010-11-2-r14.

[29] X. Mao, T. Cai, J.G. Olyarchuk, L.P. Wei, Automated genome annotation and pathway identification using the KEGG Orthology (KO) as a controlled vocabulary, Bioinformatics 21 (19) (2005) 3787–3793, https://doi.org/10.1093/bioinformatics/bti430.

[30] C. Li, Y. Zhang, R.J. Wang, J.G. Lu, S. Nandi, S. Mohanty, J. Terhune, Z.J. Liu, E. Peatman, RNA-seq analysis of mucosal immune responses reveals signatures of intestinal barrier disruption and pathogen entry following *Edwardsiella ictaluri* infection in channel catfish, *Ictalurus punctatus*, Fish Shellfish Immunol. 32 (5) (2013) 816–827, https://doi.org/10.1016/j.fsi.2012.02.004.

[31] Q.N. Liu, Z.Z. Xin, Y. Liu, D.Z. Zhang, S.H. Jiang, X.Y. Chai, Z.F. Wang, H.B. Zhang, X.G. Bian, C.L. Zhou, B.P. Tang, De novo transcriptome assembly and analysis of differential gene expression following lipopolysaccharide challenge in *Pelteobagrus fulvidraco*, Fish Shellfish Immunol. 112 (2018), https://doi.org/10.1016/j.fsi.2017.11.045.

[32] X.L. Chen, E.Y. Lui, Y.K. Ip, S.H. Lam, RNA sequencing, de novo assembly and differential analysis of the gill transcriptome of freshwater climbing perch *Anabas testudineus* after six days of seawater exposure, J. Fish. Biol. 185 (8) (2018) 153, https://doi.org/10.1111/jfb.13653.

[33] Q.Y. Wan, J.G. Su, Transcriptome analysis provides insights into the regulatory function of alternative splicing in antiviral immunity in grass carp (*Ctenopharyngodon idella*), Sci. Rep. 5 (2015) 12946, https://doi.org/10.1038/srep12946.

[34] Z.R. Han, J.F. Sun, A.J. Lv, J.A. Xian, Y.Y. Sung, X.L. Sun, X.C. Hu, K.Z. Xing, Transcriptome profiling of immune-responsive genes in the intestine of Cynoglossus semilaevis Günther challenged with Shewanella algae, Fish Shellfish Immunol. (2018), https://doi.org/10.1016/j.fsi.2018.06. 007.

[35] J.J. Zhu, C. Li, Q.W. Ao, Y. Tan, Y.G. Luo, Y.F. Guo, G.,Q. Lan, H.S. Jiang, X. Gan, Trancriptomic profiling revealed the signatures of acute immune response in Tilapia (*Oreochromis niloticus*) following *Streptococcus iniae* challenge, Fish Shellfish Immunol. 46 (2) (2015) 346–353, https://doi.org/10.1016/j.fsi.2015.06.027.

[36] C. Li, B. Beck, B.F. Su, J. Terhune, E. Peatman, Early mucosal responses in blue catfish (*Ictalurus furcatus*) skin to *Aeromonas hydrophila* infection, Fish Shellfish Immunol. 34 (3) (2013) 920–928, https://doi.org/10.1016/j.fsi.2013.01.002.

[37] L.Y. Zhu, L. Nie, G. Zhu, L.X. Xiang, J.Z. Shao, Advances in research of fish immune-relevant genes: a comparative overview of innate and adaptive immunity in teleosts, Dev. Comp. Immunol. 29 (1–2) (2013) 39–62, https://doi.org/10.1016/j.dci.2012.04.001.

[38] H. Kumar, T. Kawai, S. Akira, Pathogen recognition by the innate immune system, Int. Rev. Immunol. 30 (1) (2011) 16–34, https://doi.org/10.3109/08830185.2010.529976.

[39] F. Hayashi, K.D. Smith, A. Ozinsky, T.R. Hawn, E.C. Yi, D.R. Goodlett, J.K. Eng, S. Akirak, D.M. Underhill, A. Aderem, The innate immune response to bacterial agellin ismediated by Toll-like receptor 5, Nature 410 (2001) 1099–1103.

[40] N.T. Tran, Z.X. Gao, H.H. Zhao, S.K. Yi, B.X. Chen, Y.H. Zhao, L. Lin, X.Q. Liu, W.M. Wang, Transcriptome analysis and microsatellite discovery in the blunt snout bream (*Megalobrama amblycephala*) after challenge with *Aeromonas hydrophila*, Fish Shellfish Immunol. 45 (1) (2015) 72–82, https://doi.org/10.1016/j.fsi.2015.01.034.

[41] R.F. Lai, I. Jakovlić, H. Liu, F.B. Zhan, J. Wei, W.M. Wang, Molecular characterization and immunological response analysis of toll-like receptors from the blunt snout bream (*Megalobrama amblycephala*), Dev. Comp. Immunol. 67 (2016) 471, https://doi.org/10.1016/j.dci.2016.09.005.

[42] P.K. Jayaramu, G. Tripathi, A.P. Kumar, J. Keezhedath, M.K. Pathan, P.P. Kurcheti, Studies on expression pattern of toll-like receptor 5 (TLR5) in *Edwardsiella tarda* infected *Pangasianodon hypophthalmus*, Fish Shellfish Immunol. 63 (2017) 68–73, https://doi.org/10.1016/j.fsi.2017.01.041.

[43] F. Zhao, Y.W. Li, H.J. Pan, C.B. Shi, X.C. Luo, A.X. Li, S.Q. Wu, Expression profiles of toll-like receptors in channel catfish (*Ictalurus punctatus*) after infection with *Ichthyophthirius multifiliis*, Fish Shellfish Immunol. 35 (3) (2013) 993–997, https://doi.org/10.1016/j.fsi.2013.05.023.

[44] T. Kawai, S. Akira, The role of pattern-recognition receptors in innate immunity: update on Toll-like receptors, Nat. Immunol. 11 (5) (2010) 373–384, https://doi.org/10.1038/ni.1863.

[45] B. Verbruggen, L.K. Bickley, E.M. Santos, C.R. Tyler, G.D. Stentiford, K.S. Bateman, R.V. Aerle, De novo assembly of the *Carcinus maenas* transcriptome and characterization of innate immune system pathways, BMC Genomics 16 (1) (2015) 458–474, https://doi.org/10.1186/s12864-015-1667-1.

[46] O. Takeuchi, S.Z. Akira, Pattern recognition receptors and inflammation, Cell 140 (6) (2010) 805–820, https://doi.org/10.1016/j.cell.2010.01.022.

[47] T.S. Blackwell, J.W. Christman, The role of nuclear factor-κB in cytokine gene regulation, Am. J. Respir. Cell Mol. Biol. 17 (1997) 3–9.

[48] D.M. Rothwarf, M. Karin, The NF-κB activation pathway: a paradigm in information transfer from membrane to nucleus, Science Stke (5) (1999) 1016–1064, https://doi.org/10.1126/stke.1999.5.re1 1999.

[49] M. Zhang, Z.Z. Xiao, L. Sun, Overexpression of NF-κB inhibitor alpha in *Cynoglossus semilaevis* impairs pathogen-induced immune response, Dev. Comp. Immunol. 36 (1) (2012) 253–257, https://doi.org/10.1016/j.dci.2011.08.001.

[50] T.D. Kanneganti, M. Lamkanfi, G. Nunez, Intracellular NOD-like receptors in host defense and disease, Immunity 27 (4) (2007) 549–559, https://doi.org/10.1016/j.immuni.2007.10.002.

[51] G. Chen, M.H. Shaw, Y.G. Kim, G. Nuñez, NOD-like receptors: role in innate immunity and inflammatory disease, Annu. Rev. Pathol. 4 (4) (2009) 365–398, https://doi.org/10.1146/annurev.pathol.4.110807.092239.

[52] Y. Kadota, B. Amigues, L. Ducassou, H. Madaoui, F. Ochsenbein, R. Guerois, K. Shirasu, Structural and functional analysis of SGT1–HSP90 core complex required for innate immunity in plants, EMBO Rep. 9 (12) (2008) 1209–1215, https://doi.org/10.1038/embor.2008.185.

[53] A. Mayor, F. Martinon, T.D. Smedt, V. Pétrilli, J. Tschopp, A crucial function of SGT1 and HSP90 in inflammasome activity links mammalian and plant innate immune responses, Nat. Immunol. 8 (5) (2007) 497–503, https://doi.org/10.1038/ni1459.

[54] L.D. Church, G.P. Cook, M.F. McDermott, Primer: inflammasomes and interleukin 1β in inflammatory disorders, Nat. Clin. Pract. Rheumatol. 4 (1) (2008) 34–42, https://doi.org/10.1038/ncprheum0681.

[55] D.J.J. Waugh, C. Wilson, The interleukin-8 pathway in cancer, Clin. Canc. Res. 14 (21) (2008) 6735–6741, https://doi.org/10.1158/1078-0432.CCR-07-4843.

[56] Y.N. Mu, F. Ding, P. Cui, J.Q. Ao, S.N. Hu, X.H. Chen, Transcriptome and expression profiling analysis revealed changes of multiple signaling pathways involved in immunity in the large yellow croaker during *Aeromonas hydrophila* infection, BMC Genomics 11 (1) (2010) 506–519, https://doi.org/10.1186/1471-2164-11-506.

[57] B. Lin, S.W. Chen, Z. Cao, Y.Q. Lin, D.Z. Mo, H.B. Zhang, J.D. Gu, M.L. Dong, Z.H. Liu, A.L. Xu, Acute phase response in zebrafish upon *Aeromonas salmonicida* and *Staphylococcus aureus* infection: striking similarities and obvious differences with mammals, Mol. Immunol. 44 (4) (2007) 295–301, https://doi.org/10.1016/j.molimm.2006.03.001.

[58] S.C. Sun, S.C. Ley, New insights into NF-kB regulation and function, Cell 29 (10) (2008) 469–478, https://doi.org/10.1016/j.it.2008.07.003.

[59] H. Ha, D. Han, Y.W. Choi, TRAF-mediated TNFR-family signaling, Curr. Protoc. Immunol. (2009), https://doi.org/10.1002/0471142735.im1109ds87 11.9D.1-11.9D.14, Chapter 11.

[60] Y. Liang, Y. Zhou, P.P. Shen, NF-κB and its regulation on the immune system, Cell. Mol. Immunol. 1 (5) (2004) 343–350.

[61] B.J.H. Caamaño, C.A. Rizzo, S.K. Durham, D.S. Barton, C. Raventós-Suárez, C.M. Snapper, R. Bravo, Nuclear factor (NF)-kB2 (p100/p52) is required for normal splenic microarchitecture and B cell–mediated immune responses, J. Exp. Med. 187 (2) (1998) 185–196, https://doi.org/10.1084/jem.187.2.185.